Fermi surface and surface electronic structure of delafossite $PdCoO_2$

Kyoo Kim, Hong Chul Choi, and B. I. Min
Department of Physics, PCTP, Pohang University of Science and Technology, Pohang 790-784, Korea
(Received 7 March 2009; revised manuscript received 19 June 2009; published 15 July 2009)

We have investigated the Fermi surface (FS) and electronic structure of delafossite $PdCoO_2$. We have explored the dependence of electronic structure on the surface termination, considering both CoO_2- and Pd-terminated $PdCoO_2$ slabs. Two FS features are obtained, one larger FS from the Pd-related bulk states and the other smaller one from surface states. The bulk FS is produced mainly by the Pd $4d_{3z^2-r^2}-$Pd $5s$-hybridized state, Ψ_{d-s}, which is responsible for the high in-plane conductivity in $PdCoO_2$. The surface FS observed in angle-resolved photoemission spectroscopy is found to be produced by the hybridized Co $t_{2g}-$O $2p$ surface states for the CoO_2-terminated $PdCoO_2$. Due to the localized nature of the surface states, consideration of the spin-orbit and exchange interactions is essential to describe surface electronic structures near E_F correctly.

DOI: 10.1103/PhysRevB.80.035116 PACS number(s): 71.18.+y, 71.20.Be, 73.20.−r

ABO_2-type delafossite oxides, where A and B are, respectively, monovalent and trivalent metallic elements, exhibit variety of interesting chemical and physical properties.[1–3] They crystallize in the layered structure with the rhombohedral space group $R\bar{3}m$, which is characterized by the alternating stacking of $[BO_2]$ slabs and $[A]$ layers along the c axis to have repeated A-O-B-O layers (Fig. 1). Both the A, B cations and O anions in each layer form triangular sublattices, and B ions are located at the centers of edge-shared BO_6 octahedra. Most of delafossite oxides are insulators. In contrast, $PdCoO_2$ is a very good metal. The in-plane conductivity of $PdCoO_2$ is the highest among all the oxides and even higher than that of metallic Pd. Due to the layered structure of delafossite, $PdCoO_2$ shows highly anisotropic transport behavior.[4,5] The monovalent Pd^{1+} in $PdCoO_2$ is unique because the Pd^{1+} rarely realized in normal oxides. This occurs due to the peculiar O-Pd-O dumbbell-like linear geometry in delafossites. The $4d_{3z^2-r^2}-5s$ hybridization for the monovalent Pd was proposed to be an origin of the high metallic conductivity in $PdCoO_2$.[1,2,6]

There have been quite a few experimental[6–9] and theoretical[2,10,11] reports on the electronic structures of $PdCoO_2$. Valence-band photoemission spectroscopy (PES) study suggested that the density of states (DOS) at the Fermi level E_F comes mainly from Pd $4d$ electrons.[7] By using the augmented spherical wave band method, Eyert *et al.*[11] obtained the large electron Fermi surface (FS) centered at Γ which has hexagonal pillar shape, reflecting two-dimensional nature of $PdCoO_2$. They also reported that the metallic conductivity in $PdCoO_2$ is maintained by both the in-plane d_{xy}-$d_{x^2-y^2}$ and the in-plane part of the $d_{3z^2-r^2}$ orbitals of Pd but with a somewhat greater influence of the former. This conclusion, however, is not compatible with the existing proposal mentioned above.[1,2,6]

Angle-resolved photoemission spectroscopy (ARPES) for $PdCoO_2$ has been measured recently by Noh *et al.*[12] ARPES provides one large hexagonal-shaped FS centered at Γ in the c plane, as is consistent with the FS calculated by Eyert *et al.*[11] Interestingly, ARPES provides additional two smaller hexagonal-shaped FSs inside the larger one, which are almost degenerate to each other and rotated by $\pi/6$ with respect to the outer FS. The latter two smaller FSs are missing in the band calculation.[11] Therefore Noh *et al.*[12] suspected that these smaller FSs might originate from the surface electronic states.

In this paper, we address two main questions for $PdCoO_2$; (i) where does the seemingly additional FS feature in ARPES come from and (ii) which orbital states are responsible for the high in-plane conductivity? To identify the smaller Fermi surfaces, we have investigated the surface electronic structure of $PdCoO_2$ using the first-principle band method. Despite the intensive studies on bulk electronic structures of delafossites including $PdCoO_2$, little is known about the surface electronic structures. The surface of real material will have two kinds of termination, CoO_2- and Pd-terminated surface, with equal probability. Thus, to explore the surface electronic structure of $PdCoO_2$, we have constructed 23 and 25 atomic layer slabs for CoO_2- and Pd-terminated cases, respectively, in a hexagonal unit cell. The vacuum region is taken to be more than 15 Å (Fig. 1), which is thick enough that there is practically no interaction between two surfaces.

We have used the full-potential linearized augmented plane-wave band method[13] in the generalized gradient approximation (GGA). In general, the localized nature of surface band requires the account of effects of the spin-orbit (SO) interaction and the spin polarization. So their effects are also taken into account. Total 300 $\vec{k}$ points in the full Brillouin zone (BZ) are utilized, and, for the APW basis and the

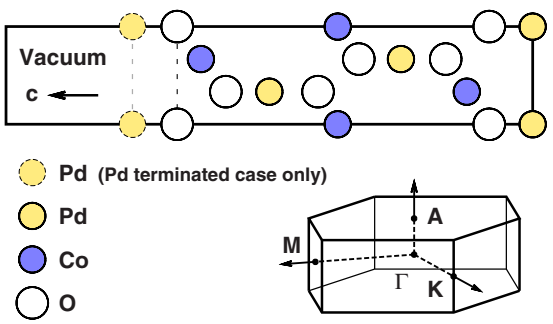

FIG. 1. (Color online) The half unit cell for the $PdCoO_2$ slab calculation. Atoms in $(11\bar{2}0)$ plane are presented. The topmost Pd layer plotted with broken line is included only for the Pd-terminated case. The BZ of hexagonal unit cell is also shown.

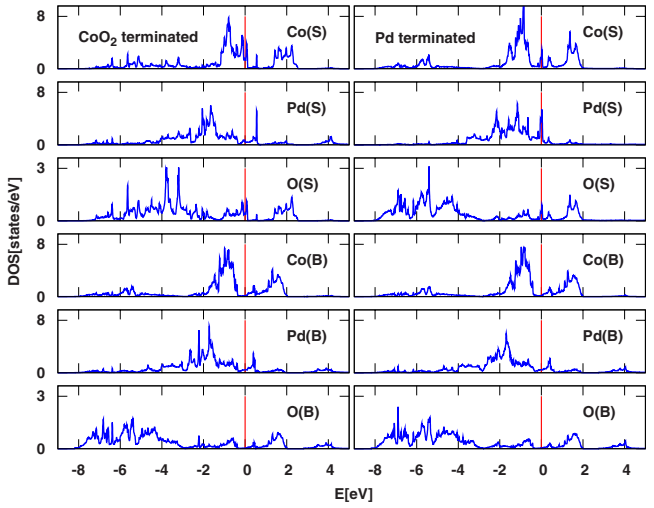

FIG. 2. (Color online) Left: the local DOS in the GGA for the CoO_2-terminated $PdCoO_2$ slab. Here (S) and (B) denote the surface-most and the bulklike deepest atoms, respectively. Right: the local DOS in the GGA for the Pd-terminated $PdCoO_2$ slab. For both, the electronic structures were obtained for the nonmagnetic phase of relaxed $PdCoO_2$ slabs.

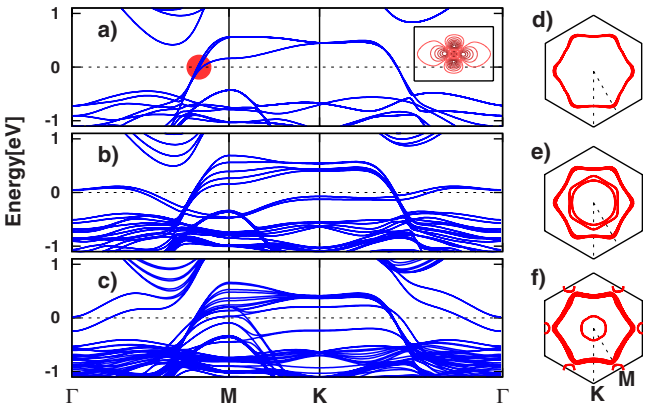

FIG. 3. (Color online) (a) Band structure near E_F for the bulk $PdCoO_2$ in the GGA. The inset is the charge-density plot in the $(11\bar{2}0)$ plane around Pd for the wave function near E_F at the red-marked $\vec{k}$. (b) Band structure near E_F for the CoO_2-terminated $PdCoO_2$. The SO interaction is included in the GGA. (c) Band structure near E_F for the Pd-terminated $PdCoO_2$. Both the SO interaction and the spin-polarization effects are included in the GGA. (d), (e), and (f) provide FSs in the first BZ for the bulk, the CoO_2-terminated, and the Pd-terminated $PdCoO_2$, respectively.

charge-density expansion, $R_{MT}K_{max}=7$ and $G_{max}=12$ are employed, respectively. To determine the surface band structure of $PdCoO_2$, one should take into account the surface relaxation properly. Comparing the surface states with and without the relaxation reveals that they are quite sensitive to the coordination and the bond length. Therefore, we have first optimized the volume and then considered the relaxation of each layer in $PdCoO_2$ slabs.

We have found that the layers at the surface are relaxed inward to the center and the size of the inward relaxation is larger for the CoO_2-terminated case than the Pd-terminated case. Accordingly, the influence of surface relaxation on the electronic structure would be larger for the CoO_2-terminated case. It is because Co $3d$ and O $2p$ bands in CoO_2 slabs are so strongly bonded that the reduced oxygen coordination at the surface will affect the surface electronic-structure substantially.

Figure 2 provides local DOSs for CoO_2- and Pd-terminated $PdCoO_2$ slabs in the GGA. It is seen that the local DOSs at the central layers for both terminations are close to each other and also consistent with those in literature.[2,10,11] This indicates the slab size in the present study is practically reasonable. For the bulklike local DOS at the central layers, the DOS between −8 to −4 eV corresponds to mainly oxygen $2p$ state, while the DOS between −4 to 0 eV corresponds to Pd $4d$ and Co t_{2g} states. Co e_g states are located above E_F in the energy range of 0–2 eV. The Pd and Co local DOSs suggest the formal valence states of Pd^{1+} and Co^{3+}, respectively. The strong covalent bonding between Co $3d$ and O $2p$ states produces the almost vanishing DOS at E_F for Co layer. Thus the metallic DOS at E_F is attributed mostly to the Pd $4d$ states. This point will be discussed further in Fig. 3(a).

At the surface, the DOS near E_F is changed remarkably. For the CoO_2-terminated case, the local DOSs of Co and O at E_F are much higher than that of Pd, indicating the formation of Co-O-related surface states. For the Pd-terminated case, the sharp peaks are prominent for all Pd, Co, and O local DOSs at E_F. The sharp surface DOS at E_F would induce the possible magnetic instability at the surface Pd. Thus we have performed the spin-polarized band calculation for the Pd-terminated $PdCoO_2$. We have indeed found that the spin-polarized state becomes more stable than the nonmagnetic state. The surface Pd has the magnetic moment of 0.4 μ_B. Co and O near the surface also have the magnetic moments of 0.1 μ_B and 0.05 μ_B, respectively. The spin polarization is negligible for layers underneath the near-surface CoO_2 layer. We performed the spin-polarized band calculation for the CoO_2-terminated case too but the magnetic moment of surface Co ion was negligible.

To examine the surface states in more detail, the band structures near E_F are presented in Fig. 3. Bulk band structure in Fig. 3(a) is consistent with that of literature.[11] The bands that cross E_F originate mainly from Pd states. These bands produce the large FS of hexagonal shape centered at Γ [Fig. 3(d)], as is again consistent with that of literature. The inset of Fig. 3(a) is the charge-density plot at Pd site for the wave function near E_F at the red-marked $\vec{k}$. The oblate shape of this charge density looks very close to that of the hybridized Pd $4d_{3z^2-r^2}$−Pd $5s$ state pointed out by Tanaka *et al.*,[6] $\Psi_{d-s}=\frac{1}{\sqrt{2}}(d_{3z^2-r^2}-s)$. This orbital feature provides clear evidence that the high in-plane conductivity in $PdCoO_2$ arises really from the large hybridization between Pd $4d_{3z^2-r^2}$ −Pd $5s$, which yields substantial metallic charge density in the interstitial region of each Pd layer [see Fig. 5(e)]. Consequently, the hybridized Pd $4d_{3z^2-r^2}$−Pd $5s$ state would contribute to the in-plane conductivity much more than planar d_{xy}-$d_{x^2-y^2}$ states. Note that this finding is contrary to that of Eyert *et al.*[11] who concluded that the metallic conductivity in $PdCoO_2$ is maintained more by the d_{xy}-$d_{x^2-y^2}$ than by the $d_{3z^2-r^2}$.

The band structure for the CoO_2-terminated case in Fig.

3(b) was obtained by considering the SO interaction in the GGA. In comparison with the bulk band in Fig. 3(a), there appears one continuous surface band near E_F along Γ-M-K-Γ which actually originates from the states of surface Co and O ions. This nearly flat surface band produces the finite DOS at E_F and the DOS peaks just above and below E_F in Fig. 2, which have Co $d_{3z^2-r^2}$ and Co d_{xy}-$d_{x^2-y^2}$ character, respectively. Note that this surface band is split, ~0.05 eV at K, by the SO interaction. Other bulk bands are not affected by the SO interaction. As shown in Fig. 3(e), these SO-split surface bands produce the smaller FSs with hole character inside the large bulk FS. Due to nearly flat nature of these surface bands, the splitting of the FSs is sizable. The $\pi/6$ rotated feature of inner FS with respect to the outer FS is ascribed to the difference in the local environment between the bulk Pd-O and the surface Co-O. Noteworthy is that the calculated FS for the CoO_2-terminated $PdCoO_2$ matches almost perfectly with the experimental FS observed by Noh *et al.*[12]

On the other hand, the band structure for the Pd-terminated case in Fig. 3(c) exhibits two kinds of surface bands near E_F, one dispersive bands around Γ comprised of Pd-Co-O orbital complexes and the other flat bands along M-K of mainly Pd 4*d* character. Both of them are split by the exchange interaction. The exchange splitting for the former amounts to 0.27 eV near Γ, and that for the latter 0.44 eV near K. As a result, besides the bulk FS, there appear two small surface FSs, electron pocket at Γ and hole pockets at M. The FS at M has the planar 4*d* character.

For ARPES experiment, the sample is prepared by cleaving. Accordingly, the statistical distribution of two kinds of terminated surfaces in ARPES will give rise to the mixture of two FSs of CoO_2- and Pd-terminated cases. However, the small FSs appeared for the Pd-terminated case are not identified in ARPES. We have mentioned above for the Pd-terminated surface that the surface bands that cross E_F near Γ are comprised of the orbitals from surface-most Pd, Co, and O ions. More specifically, they have orbital components of Pd $4d_{3z^2-r^2}$, Co $3d_{3z^2-r^2}$, and O $2p_z$ together with considerable contribution from Pd 5*s* interstitial band. This implies that these surface bands are rather delocalized, as compared to those for the CoO_2-terminated case. Note that the PES intensity is weaker for more dispersive band. The unidentified small electron pocket FS around Γ in ARPES experiment might be due to this rather delocalized feature of the Pd-terminated surface states. Another possible explanation for the absence of FSs from Pd-terminated surface states is the probable hydrogen absorption to the Pd surface, which would eliminate the surface states. This aspect needs further investigation.

The formation of the surface states can be understood as shown in Fig. 4. In an ionic bonding model, Pd and Co in $PdCoO_2$ donate one and three electrons to oxygen ion, respectively. For the CoO_2-terminated case in Fig. 4(a), the surface oxygen cannot receive an electron from missing upper Pd. In compensation, the surface oxygen will take more electron from underlying Co. This mechanism leads to the upward shift of the Co t_{2g} band at the surface, which otherwise was below E_F, so as to produce the nearly flat metallic surface band in Fig. 3(b). On the other hand, for the Pd-terminated case in Fig. 4(b), the surface Pd do not need to donate electron to missing upper oxygen. Then the Pd band at the surface becomes more occupied and shifts down to yield the almost filled surface band along M-K in Fig. 3(c).

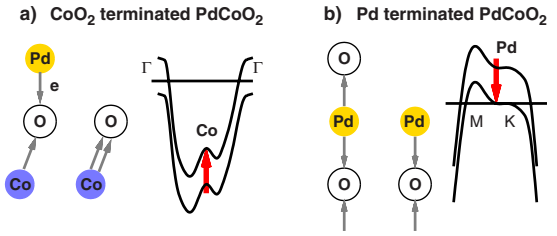

FIG. 4. (Color online) The schematic model for the formation of surface states in $PdCoO_2$. The change in the charge transfer and the consequent band shift at the surface are plotted. (a) For the CoO_2-terminated case, the Co-related band is shifted up. (b) For the Pd-terminated case, the Pd-related band along M-K is shifted down.

Figure 5 presents the charge-density difference (CDD) plots for the CoO_2-terminated $PdCoO_2$ slab, which are obtained by subtracting the superposed atomic charge density from the calculated total charge density. The CDDs are plotted in the $(11\bar{2}0)$ plane and also at each Co and Pd layer. These plots provide the information on the charge redistribution in solid from the atomic charge density, the charge transfer from cations to O ion, and the difference between bulk and surface charge densities. The CDD plot at the central bulklike Pd layer [Fig. 5(e)] shows that there are electrons which are distributed uniformly in the interstitial region. Note that the red solid line in the interstitial region represents the positive charge density. These delocalized electrons produce the metallic behavior in $PdCoO_2$. The CDD plot at the near-surface Pd layer [Fig. 5(c)] also exhibits delocalized electrons in the interstitial region. In fact, we have found that the metallic nature at the near-surface Pd layer is stronger than that at the central Pd, suggesting that the conductivity would be higher at the near-surface Pd layer. The plot in the $(11\bar{2}0)$ plane manifests that the metallic electrons in the interstitial region of Pd layers form apparent layer structures. On the other hand, the CDD plots at the Co layers exhibit

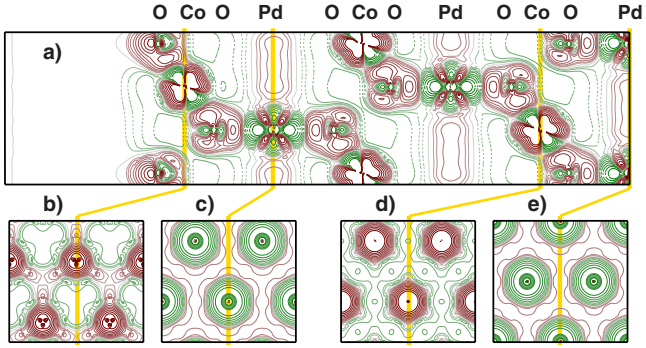

FIG. 5. (Color online) (a) CDD in the $(11\bar{2}0)$ plane for the CoO_2-terminated $PdCoO_2$. (b), (c), (d), and (e) are CDDs at the surface Co, the near-surface Pd, the near center Co, and the central Pd layers, respectively. Log scale is used in the contour plot. Red solid and green broken lines represent the positive and the negative CDD, respectively.

very distinct feature between the surface and bulklike Co. At the bulklike Co layer [Fig. 5(d)], electrons are localized (CDD is negative in the interstitial region) to have insulating nature, whereas, at the surface Co layer [Fig. 5(b)], there appear some electrons in the interstitial region which link Co and O. Actually these delocalized electrons produce the inner surface Fermi surfaces in Fig. 3(e).

In the CDD around Co in Fig. 5(a), the Co charge density pointing toward oxygen at each octahedral corner is drawn with the green broken lines (negative CDD). This indicates that the Co e_g-like orbital in the local coordinate is unoccupied. Similarly, in the CDD around Pd, the Pd charge density pointing toward oxygens above and below is negative, implying that the Pd $4d_{3z^2-r^2}$-like orbital is unoccupied. The prolate shape of this green part of Pd orbital resembles another Pd $4d_{3z^2-r^2}-$Pd $5s$-hybridized state, $\Psi_{d+s}=\frac{1}{\sqrt{2}}(d_{3z^2-r^2}+s)$, mentioned by Tanaka *et al.*[6] Because of the crystal field from O ion, Ψ_{d+s} is higher in energy than Ψ_{d-s}. This unoccupied orbital forms the nearly flat bulk Pd band at $\sim$0.5 eV above E_F along M-K in Fig. 3, in which some Co e_g and O $2p_z$ states are mixed together. Due to the prolate nature, Ψ_{d+s} is hybridized strongly with O $2p_z$, producing complex peak structures in the DOS. For example, the peak at $\sim$4 eV in the Pd(B) and O(B) PDOSs in Fig. 2 corresponds to an antibonding state between them.

In conclusion, we have found that the FSs in delafossite $PdCoO_2$ originate from the surface states as well as the bulk states. The bulk states at E_F correspond to the Pd $4d_{3z^2-r^2}-$Pd $5s$-hybridized states (Ψ_{d-s}), which are responsible for the high in-plane conductivity in $PdCoO_2$. The surface FS for the CoO_2-terminated surface arise from the hybridized Co $t_{2g}-$O $2p$ states. For the Pd-terminated surface, the electron pocket FS at Γ and hole pockets at M arise from Pd-related surface states. Due to the localized nature of surface states, the SO interaction and the exchange interaction turn out to be important to describe surface electronic structures near E_F for the CoO_2- and Pd-terminated cases, respectively. The FSs determined from ARPES experiment are perfectly in agreement with those obtained theoretically for the CoO_2-terminated surface. In contrast, the FSs from Pd-terminated surface states are missing in ARPES.

This work was supported by the KOSEF/MEST (Grant No.2009-0079947). We thank H.-J. Noh, H.-D. Kim, and S. C. Jung for useful discussions.

[1] R. D. Shannon, D. B. Rogers, and C. T. Prewitt, Inorg. Chem. **10**, 713 (1971).
[2] R. Seshadri, C. Felser, K. Thieme, and W. Tremel, Chem. Mater. **10**, 2189 (1998).
[3] M. A. Marquardt, N. A. Ashmore, and D. P. Cann, Thin Solid Films **496**, 146 (2006).
[4] M. Tanaka, M. Hasegawa, and H. Takei, J. Phys. Soc. Jpn. **65**, 3973 (1996).
[5] H. Takatsu, H. Takatsu, S. Yonezawa, S. Mouri, S. Nakatsuji, K. Tanaka, and Y. Maeno, J. Phys. Soc. Jpn. **76**, 104701 (2007).
[6] M. Tanaka, M. Hasegawa, T. Higuchi, T. Tsukamoto, Y. Tezuka, S. Shin, and H. Takei, Physica B **245**, 157 (1998).
[7] T. Higuchi, T. Tsukamoto, M. Tanaka, H. Ishii, K. Kanai, Y. Tezuka, S. Shin, and H. Takei, J. Electron Spectrosc. Relat. Phenom. **92**, 71 (1998).
[8] M. Hasegawa, I. Inagawa, M. Tanaka, I. Shirotani, and H. Takei, Solid State Commun. **121**, 203 (2002).
[9] T. Higuchi, M. Hasegawa, M. Tanaka, H. Takei, S. Shin, and T. Tsukamoto, Jpn. J. Appl. Phys. **43**, 699 (2004).
[10] H. Okabe, M. Matoba, T. Kyomen, and M. Itoh, J. Appl. Phys. **93**, 7258 (2003).
[11] R. Eyert, R. Frésard, and A. Maignan, Chem. Mater. **20**, 2370 (2008).
[12] H.-J. Noh, J. Jeong, J. Jeong, E.-J. Cho, S. B. Kim, K. Kim, B. I. Min, and H.-D. Kim, Phys. Rev. Lett. **102**, 256404 (2009).
[13] M. Weinert, E. Wimmer, and A. J. Freeman, Phys. Rev. B **26**, 4571 (1982); H. J. F. Jansen and A. J. Freeman, *ibid.* **30**, 561 (1984).